

## Flattening spacetime near the Earth

Robert L. Forward

*Hughes Research Laboratories, 3011 Malibu Canyon Road, Malibu, California 90265*

(Received 18 January 1982)

Experimental regions where all forces are minimized are desired for many types of space experiments such as those involving gravity measurements and materials processing. In a free-fall orbit, the gravity acceleration force of the Earth is canceled to first order by the orbital motion. The cancellation, however, is perfect only at the center of mass of the freely falling object. At the other points in the object there will be accelerations induced by the gravity gradient tides of the Earth. These can cause acceleration forces of  $10^{-7}$  m/sec<sup>2</sup> (10 nanogravities) at a distance of only 3 cm from the center of mass and proportionately larger accelerations at greater distances. We show that if we place six 100-kg spheres in a ring whose plane is orthogonal to the local vertical and whose center is at the center of mass of the experiment, the gravity attraction of the spheres will produce a counter-tide that can reduce the Earth tide accelerations by factors of 100 or more in significant experiment volumes. We give an example where we produced calculated acceleration levels below  $10^{-11}$  m/sec<sup>2</sup> (1 picogravity) over a disk-shaped experiment volume 30 cm in diameter and 20 cm thick in a geostationary orbit space laboratory. In materials-processing experiments, the acceleration levels attainable will be limited by the self-gravity of the material being processed. Typical self-gravity acceleration levels are 1–100 nanogravities near the outer surface of batches of moderately dense materials a number of centimeters in size. The self-gravity of a disk-shaped sample can be reduced by first using “guard rings” and “guard caps” to smooth out edge effects. Then a combination of gravity gradients from two massive spheres and rotation of the sample can be used to null the self-gravity everywhere inside the sample disk. We give an example where the maximum surface acceleration in a disk of water 30 cm in diameter and 10 cm thick in geostationary orbit is reduced by a factor of 2000 from  $3 \times 10^{-8}$  m/sec<sup>2</sup> (3 nanogravities) to  $1.3 \times 10^{-11}$  m/sec<sup>2</sup> (1.3 picogravities). Since the gravity gradient forces in a region are manifestations of the Riemann curvature of spacetime caused by the mass of the Earth and the self-mass of the experiment, these techniques for reducing the gravity forces in a region can be thought of as a method for “flattening” a region of spacetime—even a region that has mass in it.

### I. INTRODUCTION

There are a number of future space experiments that to be successful will require an environment with very low residual force levels. Some are gravity experiments, such as a gravitational clock to measure the Newtonian gravity constant or a free-fall Eotvos experiment to test the equivalence of gravitational and inertial masses. Others are drag-free satellite experiments to study aerodynamics, map the gravity fields of the earth, and search for gravity waves. Then there are advanced materials-processing payloads proposed for future orbital missions that will require a low-acceleration environment. The desired acceleration levels for all these experiments range from  $10^{-5}$  m/sec<sup>2</sup> (microgravities) on down.

Achieving these low-acceleration levels in a space laboratory in low Earth orbit will be very difficult. If the payload is attached to the spacecraft, then the rotations, accelerations, vibrations, and gravity attraction of the spacecraft will induce significant accelerations on any experiment package, even if the package is at the center of mass of the vehicle. Manned spacecraft are especially troublesome. For example, a sneeze by a crewmember in a 100-ton spacecraft will induce an acceleration level of  $10^{-3}$  m/sec<sup>2</sup> (0.1 milligravity).<sup>1</sup>

To even begin approaching ultralow acceleration levels in an experiment, it will be necessary to allow the experimental package to float freely within a vacuum chamber. Depending upon the size of the chamber and the residual spacecraft accelerations, a number of minutes of drag-protected free-

fall time can be obtained this way before the experiment package contacts the walls of the chamber. For longer experiment times, the spacecraft and its chamber would have to be operated in a "drag-free" mode.<sup>2</sup> In drag-free operation, there are sensors in the chamber monitoring the position of the floating experiment package and controlling the spacecraft thrusters to maintain the chamber centered about the experiment package.

Once the experiment is in free-fall in a vacuum chamber, and adequately protected from such things as light pressure and electric and magnetic fields, then the only perturbing accelerations left to bother the experiment are those due to gravity and inertia. These residual gravity and inertial accelerations come from the gravity gradient tide of the Earth, the gravity gradients from nearby masses in the spacecraft, the self-gravity of the experiment itself, and centrifugal acceleration due to any rotation of the experiment package.

We will show how we can reduce those residual gravity accelerations by a number of techniques, achieving reductions in residual gravity accelerations by factors of over 1000.

## II. SPACECRAFT GRAVITY GRADIENT FIELDS

There will be some experiments where the residual acceleration due to self-gravity is not a significant problem. This could happen in a materials-processing experiment where the amount of material is small, or in gravity experiments where the self-gravity is part of the experiment (the gravitational clock), or in experiments where the bodies involved are rigid and it is only the accelerations of the body as a whole that are of concern (the detecting mass in a laser interferometer gravity radiation experiment). In these cases, the major source of undesired accelerations on the experiment will be due to the gravity gradient tides of the Earth and the gravity gradients of the spacecraft. (We are assuming that good experimental procedure will prevent any undesired rotation of the experiment package that would produce unwanted centrifugal accelerations.)

By proper design of the low-gravity vacuum chamber (basically a spherical shape with three-axis symmetry in the placement of ports, attachment fixtures, etc., to minimize the gravity gradients at the center of the chamber) and by proper placement of the chamber at a distance from large and variable masses such as fuel tanks and moving platforms, the gravity gradients from the space-

craft can be kept small compared to the gravity gradients of the Earth. The two gravity fields will then combine to produce one gravity gradient field in the chamber with the major tension axis nearly along the local vertical, the two compression axes nearly normal to the local vertical, and the strength of the components nearly equal to those of the Earth for that orbital altitude. The problem of compensation is then reduced to the problem of compensating the gravity gradient field of the Earth.

## III. GRAVITY GRADIENT OF THE EARTH

The gravity gradient tides of the Earth are the components of a second-rank tensor. As shown in Fig. 1, if the coordinate system used to measure the gravity gradient tensor is oriented so that one axis is aligned along the local vertical, then the principal components of the Earth gravity gradient are those along the diagonal of the tensor:

$$\Gamma_{ij} = \begin{pmatrix} \Gamma_{XX} & \Gamma_{XY} & \Gamma_{XZ} \\ \Gamma_{YX} & \Gamma_{YY} & \Gamma_{YZ} \\ \Gamma_{ZX} & \Gamma_{ZY} & \Gamma_{ZZ} \end{pmatrix} \approx \begin{pmatrix} \Gamma_H & 0 & 0 \\ 0 & \Gamma_H & 0 \\ 0 & 0 & \Gamma_V \end{pmatrix}. \quad (1)$$

The two components consist of a tension along the vertical axis given by the equation

$$\Gamma_V = \frac{+2 GM}{(R+h)^3} \quad (2)$$

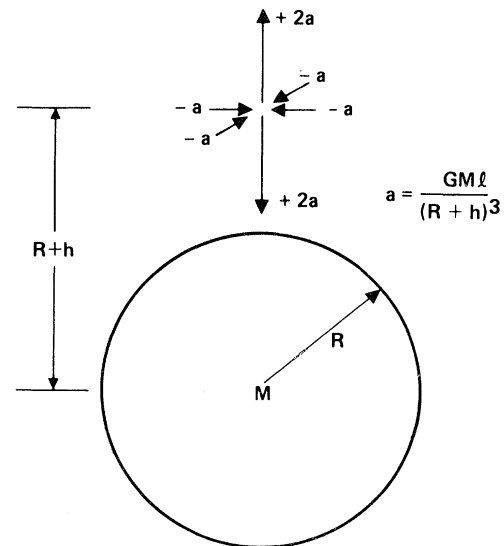


FIG. 1. Gravity gradients.

and a nearly uniform compression normal to the local vertical given by the equation

$$\Gamma_H = \frac{-GM}{(R+h)^3}, \quad (3)$$

where  $M$  and  $R$  are the mass and radius of the Earth, respectively, and  $h$  is the orbital altitude. Since the Earth is not spherically symmetric, there will be slight variations in these principal components, and the off-diagonal terms will not be strictly zero, indicating a slight tilt of the gravity gradient tensor with respect to the local gravity vertical. At the probable altitudes where our ultralow-gravity compensation techniques will be used (in synchronous orbit, or at least well out of the Earth's atmosphere) these variations will be small. In any case, the variations can also be compensated for by minor modifications to the compensation techniques we will discuss. For the rest of the paper we will assume we have a spherical Earth and that the gravity gradient field of the Earth is aligned along the local gravity vertical with the three principal components given by Eqs. (2) and (3).

The gravity gradient of the Earth will induce accelerations in a freely falling object at any point that is not at the center of mass of the object. The induced accelerations level is just the scalar product of the gravity gradient tensor times the position vector of the point  $l^j$  and is given by

$$a_i = \Gamma_{ij} l^j, \quad (4)$$

For a point at a distance  $l$  above the center of mass along the axis of the local vertical, the resulting vertical acceleration is upward and given by

$$a_v = \frac{+2 GM l}{(R+h)^3}. \quad (5)$$

In a 5000-km orbit, the accelerations caused by the Earth gravity gradient at a distance of 1 m are about  $2 \times 10^{-6}$  m/sec<sup>2</sup> (0.2 microgravities), while at 36,000 km (geostationary orbit) it has dropped to 1.1 nanogravities.

#### IV. GRAVITY GRADIENT COMPENSATOR

To counteract the gravity gradient field of a nearby massive body such as the Earth, we propose the use of six dense spheres placed in a ring normal to the local vertical and surrounding the experimental region to be compensated. By varying the radius of the ring of masses we can vary the amount of compensation. The gravity gradient

pattern at the center of such a collection of masses is shown in Fig. 2. Note that near the center of the ring the vertical component has a magnitude that is twice that of the two horizontal components, just as the Earth's gradient field does, while the directions of the ring gradient field are reversed compared to the Earth's gradient field. (As an interesting side note, the tensor gravity gradient field produced at the center of the ring is equivalent to the field that would be produced by a *negative* mass placed below the center point.)

The strength of the gravity gradient at the center depends not only on the combined mass of the spheres, but also on the radius of the circle. For six spheres of mass  $m$  in a ring of radius  $r$ , the combined gravity gradient in the vertical direction is

$$\gamma_V = \frac{-6Gm}{r^3}, \quad (6)$$

while in the plane of the ring the horizontal field is nearly uniform and near the center is given by

$$\gamma_H = \frac{+3Gm}{r^3}. \quad (7)$$

Actually, any ring-shaped collection of masses will produce this inverse gravity gradient pattern at the center. A solid ring would produce an axially symmetric pattern, but it would be difficult to change the radius of the ring to compensate for the various gravity gradients at different altitudes. Four masses will suffice for the ring, but we have found that six masses produce a substantially larger compensated volume of low gravity about the central point, while more than six masses do not increase the compensated volume significantly.

This design for a gravity gradient compensator was originally conceived for use in a science fiction novel<sup>3,4</sup> as a method for protecting a manned

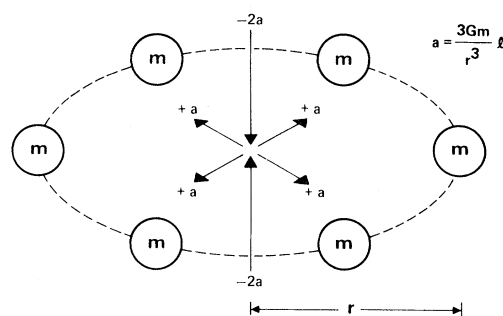


FIG. 2. Gravity gradients of a six-sphere tidal compensator ring.

spaceship in a 400-km-high orbit around a neutron star. The tides at 400 km from a neutron star are 200 gravities per meter, enough to literally tear a person apart. In this paper we propose a less exotic version of the gravity gradient compensator in order to keep delicate experiments from being “torn apart” or perturbed by the much milder tides of the Earth.

To provide as large an interior region as possible for the experiment, it is desirable to make the compensator spheres massive and dense. For the purposes of this paper we have arbitrarily chosen each compensator sphere to be 100 kg in mass and made of a dense material such as depleted uranium (density of 18 700 kg/m<sup>3</sup>) or tungsten (19 300 kg/m<sup>3</sup>). The radius of a 100-kg sphere with these densities is about 11 cm.

To determine the ring spacing for the six spheres so that their gravity gradient field will compensate the gravity gradient of the Earth, we set the sum of the vertical gravity gradient of the Earth [Eq. (2)] and the vertical gravity gradient of the six spheres [Eq. (6)] to zero:

$$\Gamma_V + \gamma_V = 0 = \frac{2GM}{(R+h)^3} - \frac{6Gm}{r^3}. \quad (8)$$

Solving this for the ring spacing  $r$  produces the equation

$$r = \left[ \frac{3m}{M} \right]^{1/3} (R+h). \quad (9)$$

To provide exact compensation at the center of the ring in a 5000-km orbit requires a ring radius of 42 cm, giving a working area of 62 cm diameter, while in geostationary orbit, the ring radius is 1.56 m, giving almost 3 m of working room.

The match of the compensator tides to the Earth tides is only perfect at the exact center of the ring of compensator spheres. As is shown in Fig. 3, however, there is a substantial region about the center point where the match of the two fields is close enough so that a significant reduction in the accelerations caused by Earth tides can be produced. Figure 3 assumes an orbital altitude of 5000 km and a compensator ring radius of 42 cm. The dashed lines are the acceleration levels due to the Earth tides at various distances from the center. The upper dashed line shows the vertical accelerations along the central axis and the lower dashed line shows the horizontal accelerations in the central plane orthogonal to the vertical axis. Note the vertical gradient of  $5.39 \times 10^{-7} \text{ sec}^{-2}$  (+ 0.55 nanogravities/cm) is twice the horizontal gradient. For any point not on the vertical axis or

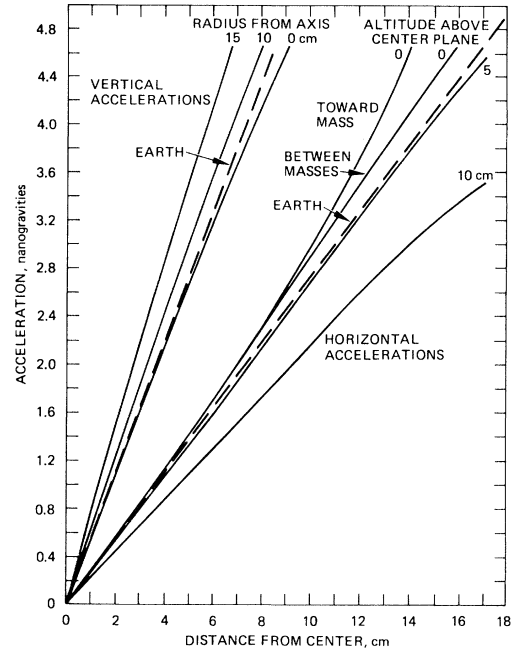


FIG. 3. Comparison of gravity gradients from Earth and compensator ring.

in the horizontal plane, the acceleration vector will be the vector sum of the corresponding vertical and horizontal values.

Also plotted in Fig. 3 are the accelerations due to the compensator. For the vertical accelerations along the central axis we see that the compensator accelerations match those of the Earth well out to 5 to 7 cm. The match is still good for vertical paths paralleling the central axis out to a 10-cm radius from the center.

For the horizontal accelerations, the match in the horizontal plane is good out to about 10 cm and stays matched well in planes 5 cm above and below the central plane. Because of our choice of six spheres instead of a ring for the shape of the compensator structure, the fields produced by the compensator have hexagonal symmetry. As we can see by the upper two horizontal acceleration traces, the fields along directions that slice through a mass are slightly different than the fields along directions that pass between two masses.

## V. RING COMPENSATOR OF EARTH GRAVITY GRADIENTS

If we place the compensator ring around the experimental region to be shielded from the Earth tides and adjust the ring spacing to null the Earth gravity gradients at the center, we will find that

the residual acceleration contours will have the shape of a thick disk.

The residual acceleration contours at the center of a ring of compensator spheres with a radius of 156 cm in a space laboratory in a 36 000-km amplitude geostationary orbit are shown in Fig. 4. The outer contour, with a residual acceleration of 10 picogravities, represents a reduction of 30 in acceleration over a volume some 60 cm in diameter and 50 cm thick. The inner contours of 1 picogravity and 100 femtogravities represent regions where the Earth gravity gradient accelerations are compensated by factors of 130 and 550, respectively. With this amount of compensation we have reached a remarkably low level of acceleration. At 100 femtogravities, it would take an atom 10 sec to fall its own diameter.

When we reach this level of tidal compensation, the varying or unknown gravity gradients induced by masses in the spacecraft will become important. For example, a heavy-set (100 kg) experimenter at 11 m distance will induce a gravity gradient of  $10^{-11} \text{ sec}^{-2}$  at the site of the experiment, and that will produce 100 femtogravities acceleration at 10 cm distance from the center of the experiment. (The  $10^{-13} \text{ sec}^{-2}$  tides of the moon and sun, however, are too small to be of concern.) If such levels of residual acceleration are desired, the experimental chamber will probably have to be guarded with an array of gravity gradient sensors<sup>5</sup> that will monitor the actual gravity gradient field in the region of the experiment chamber and adjust the radius and tilt of the compensator ring accordingly.

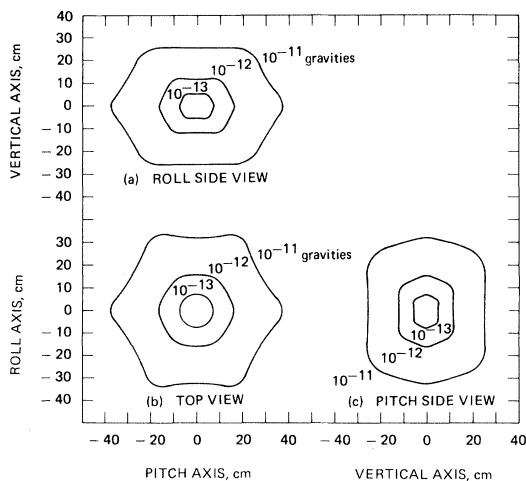


FIG. 4. Residual acceleration contours for compensated Earth gravitational gradients at synchronous orbit altitude.

## VI. SELF-GRAVITY ACCELERATIONS

At the low-gravity levels that we are striving for, the ultimate limit would seem to be the self-gravity of the material used to build the experimental apparatus itself. This is not always the case, for there are experiments where the self-gravity is part of the experiment. One example would be a gravitational “clock” experiment to compare “gravitational” time with “hydrogen atom” time. This would involve a ball bouncing back and forth inside a hole drilled through a massive sphere. In other experiments, the self-gravity is not important. These would be experiments using a piece of apparatus such as a free-fall Eotvos balance to compare the ratio of gravitational to inertial mass for different substances. Here, careful control of the geometry of the massive portions will produce a null gravity effect on the torsion sensing portions of the apparatus.

There are other experiments, however, that will have to contend with self-gravity. Examples are materials-processing experiments on containers of liquids, such as melted exotic alloys or foamed metals. In these experiments we have a container many centimeters across and wish to keep the acceleration levels—including the self-gravity induced acceleration field—to as low a level as possible throughout the sample, while maximizing the volume.

Self-gravity induced accelerations become important when we want to achieve nanogravity levels of acceleration. For example, a sphere of water 10 cm in radius has a self-gravity induced acceleration at its surface of 3 nanogravities. It is possible, however, to cancel the self-gravity of a sample to produce a low-gravity region throughout the whole volume. To do this we first use “guard rings” and “guard caps” of similar density material to reduce the “edge effects” in the self-gravity field. We then use a combination of gravity gradients from massive spheres and rotation of the sample to counteract the self-gravity field. We have found that the best shape for the sample volume to be compensated is a disk.

## VII. SELF-GRAVITY FIELD OF A DISK

The self-gravity field inside and outside a massive “thick” disk is quite complicated. Simple analytical solutions exist only along paths of high symmetry. For example, the vertical components of the self-gravity field of a disk of density  $\rho$ ,

thickness  $2t$ , and radius  $r$  at a point  $l$  along the axis of the disk is given by<sup>6</sup>

$$a_d = 2\pi G\rho \{ [(l+t)^2 + r^2]^{1/2} - [(l-t)^2 + r^2]^{1/2} - 2l \}, \quad (10)$$

if the point is inside the disk, and by

$$a_d = 2\pi G\rho \{ [(l+t)^2 + r^2]^{1/2} - [(l-t)^2 + r^2]^{1/2} \pm 2t \}, \quad (11)$$

if the point is outside the disk. The negative sign before the term  $2t$  is to be taken if  $l$  is positive and the positive sign if  $l$  is negative. For an infinitely thin disk, Eq. (10) for the acceleration inside the disk reduces to

$$a_d = -4\pi G\rho l \quad (l \leq t). \quad (12)$$

Thus, for any given density of the disk, there is a linear increase in inward acceleration with increasing distance from the center until the surface of the disk is reached.

The acceleration field inside a real massive disk due to its self-gravity is axially symmetric, but at points away from the central axis it varies considerably from the relative of Eq. (10). We have programmed a computer to calculate the gravity forces at any point inside or outside the massive disk by replacing the disk with a collection of mass points. For our attempts to compensate the self-gravity forces in a materials-processing experiment, we arbitrarily chose a nominal sample volume consisting of a disk of material with the density of water that is 30 cm (1 ft) in diameter and 10 cm (4 in.) thick. The computer-calculated field of this nominal sample volume agrees quite well with Eq. (10), although there is a slight variance of 0.05 nanogravities (1.7%) as we near the top surface of the disk. This indicates that our computer mass model is an adequate representation of a real disk.

The calculated self-gravity acceleration fields along selected paths in our sample volume are shown in Fig. 5. One trace shows the change in vertical acceleration as we move from the center up along the axis of symmetry. We see the almost linear increase predicted by Eq. (10) with a slight curvature as we approach the top surface of the disk. A similar trace taken along the vertical direction but out on the rim 15 cm away, also gives a nearly linear increase in vertical acceleration as we move in the vertical direction, but the amplitude of the acceleration is nearly half that at the center, showing the "edge effects" of the "missing mass" outside the rim boundary.

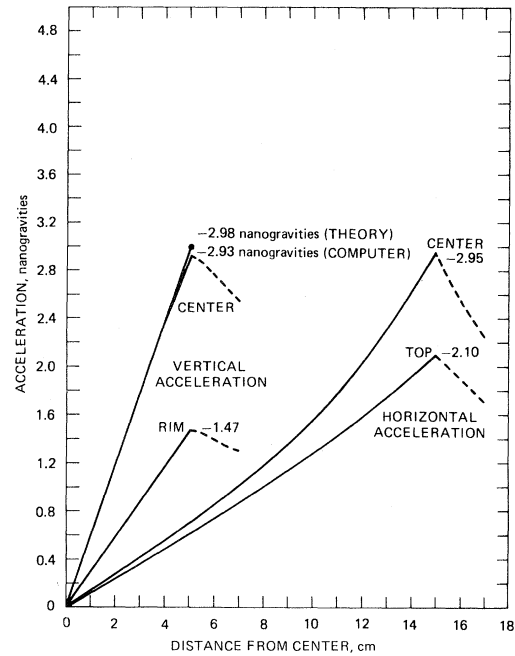


FIG. 5. Computed self-gravity induced accelerations in nominal sample disk.

For the horizontal acceleration we see a similar increase with increasing distance. In Fig. 5, the upper horizontal curve is for a path that starts at the center of the disk and moves radially outward toward the rim. The curve starts out with a linear trend, but as it approaches the rim there is a definite curvature to the acceleration trend. We get a similar, but lower amplitude curve if we choose a path that starts at the top of the disk, 5 cm up from the center, then goes radially out from there to the edge of the disk.

The self-gravity field in our nominal sample disk is seen to vary considerably over the volume, and at first glance it would seem that it would be difficult to compensate this highly irregular field to any degree of accuracy. However, just as is done in electrostatics when making highly accurate standard capacitors for absolute capacitance measurements, we can smooth out these variations by adding guard rings of similar density material to eliminate the edge effects.

### VIII. GUARD RINGS AND GUARD CAPS

The guard rings for our disk-shaped nominal materials-processing sample will be ring-shaped chambers of the same thickness as the sample disk,

surrounding the disk and containing material with a density equal to that of the sample material (see Fig. 6). The chamber containing the guard ring material should be separated by a thin wall from the material in the sample, since the material in the guard ring will be subjected to uncompensated accelerations and will have nonuniform forces on it. If it is a liquid, it will be flowing, and we do not want the current flows to disturb the material in the compensated volume.

To illustrate the improvement in field uniformity obtained by the use of a guard ring, we calculated the acceleration forces inside the disk sample for guard rings of larger and larger width. The thickness of the guard rings is kept constant at the 10-cm thickness of the disk sample. The upper curves in Fig. 7 shows the vertical accelerations with increasing vertical distance for paths at the center and at the outer rim 15 cm away. Notice that even a 10-cm guard ring added to the disk brings the acceleration levels for the center and rim within 10% of each other. The addition of a 30-cm-wide guard ring that triples the size of the 15-cm-radius disk sample to 45 cm, is sufficient to make the vertical acceleration field uniform to within about 1% over the entire disk. Notice in Fig. 7 that as the guard ring is made larger and larger, the amplitude of the vertical acceleration increases. In the extreme case of an infinitely large guard ring, the acceleration level would approach the limit given by Eq. (12) for an infinitely thin disk.

The addition of the guard ring also makes the horizontal accelerations inside the disk sample more uniform. In the lower curves of Fig. 7 we can see that with increasing guard-ring radius the

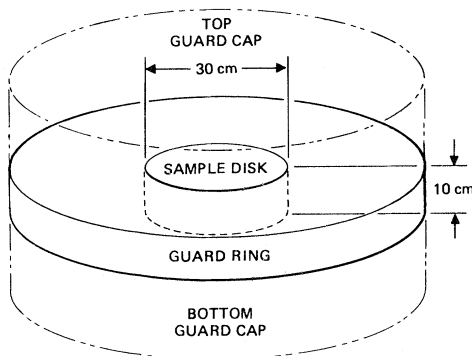


FIG. 6. Sample disk with guard ring and guard caps.

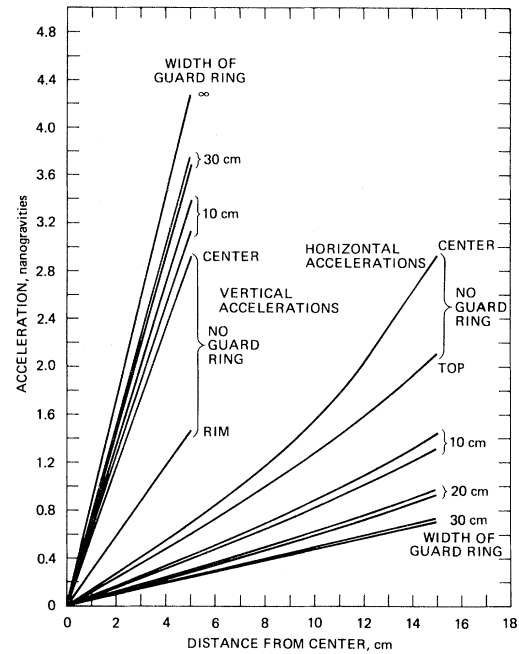


FIG. 7. Accelerations in sample disk with guard ring.

variations between the horizontal accelerations at the center and top of the disk become smaller and the curvature of the acceleration field becomes less pronounced. Even with a 30-cm guard ring, however, there is still a definite upward curvature to the trace. Also notice, that while adding to the radius of the guard ring *increases* the vertical acceleration levels, it causes a *decrease* in the horizontal acceleration levels.

In addition to studying the effects of guard rings, we also investigated the effect of adding "guard caps" of material on the top and bottom of the disk (see Fig. 6). These would be cylinders with the same diameter as the disk (or the disk plus guard ring) with material of the same density as the sample material. We found that just as in the case of adding a guard ring, the addition of guard caps makes the acceleration field in the sample volume more uniform. However, while adding a guard *ring* makes the vertical acceleration *increase* in amplitude while becoming more uniform, the addition of a guard *cap* causes the vertical acceleration to *decrease* in amplitude while becoming more uniform. This effect is important, as we shall later use this vertical acceleration decrease effect to lower the amplitude of the inward vertical acceleration before we try to compensate it with the outward gravity gradient tidal accelerations from a gravity gradient generator.

### IX. GRAVITY GRADIENT GENERATOR

The gravity gradient generator consists of two dense masses, nominally 100-kg spheres, one on each side of the sample volume and aligned along the axis of the disk. Because the two spheres are equal in mass, their gravity field cancels out at the center point half way between them. What is left are the tidal forces of the two masses as is shown in Fig. 8.

For two spheres of mass  $m$  spaced a distance  $2r$  apart, the gravity gradient field produced at the center is given by a second-rank tensor,

$$g_{ij} = \begin{pmatrix} g_H & 0 & 0 \\ 0 & g_H & 0 \\ 0 & 0 & g_V \end{pmatrix}, \quad (13)$$

where the vertical component is a tension given by

$$g_V = \frac{+4Gm}{r^3} \quad (14)$$

and the horizontal components are a compression

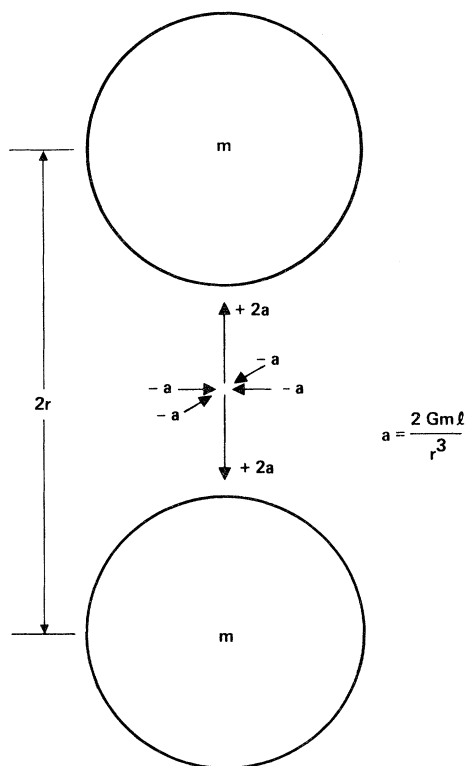


FIG. 8. Gravity gradients of a two-sphere tidal augmentor.

given by

$$g_H = \frac{-2Gm}{r^3}. \quad (15)$$

These values for the strength of the gravity gradient are only strictly valid right at the central point, but they remain close to these values for a significant region about the central point. Note that the strength and directional characteristics of the generator tides are similar to those of the Earth tides.

### X. EXAMPLE OF SELF-GRAVITY COMPENSATION IN GEOSTATIONARY ORBIT

Although the following techniques will work at any orbital altitude, the job of making an acceleration-free region becomes somewhat simpler if you are in a geostationary orbit about the Earth. As an example of compensating the gravity fields everywhere *inside* a massive body, let us start with our nominal 30-cm diameter by 10-cm thick disk-shaped container containing, for example, some pharmaceutical being purified by electrophoresis. As we saw in Fig. 5, the self-gravity of this disk is quite nonuniform and reaches some 3 nanogravities near the outer surface. We will assume the disk is inertially stabilized.

We first want to remove the residual background gravitational gradient fields from the Earth and nearby masses. If we assume that the space station is stabilized in an Earth-pointing orientation, then the spacecraft gradients and the Earth gradients will combine into a single gravity gradient field that is fixed with respect to the Earth, but rotates once per orbit with respect to inertial space. This combined background gradient will be dominated by the Earth gradient. At geostationary orbit altitude, the Earth gravity gradient cause acceleration levels in the disk of some 80 picogravities. As we showed before, a set of six 100-kg gravity gradient compensator masses spaced in a ring of 1.56 m radius will reduce these background gradient-induced accelerations to less than 2 picogravities. This acceleration level is some 1500 times smaller than the 3-nanogravity accelerations induced by the self-gravity of the disk.

Since the compensator masses stay fixed relative to the Earth, they rotate once per orbit with respect to the inertially stabilized sample disk. The residual gravity contours are no longer the disk-shaped contours of Fig. 4, but slightly smaller cylindrically shaped regions obtained by rotating



the shapes of Fig. 4 about the roll or pitch axis.

With the background accelerations reduced to picogravity levels, we now attack the nanogravity accelerations induced by the self-gravity. We start with the vertical component of the self-gravity. As we see in Fig. 9, the self-gravity accelerations of the disk alone vary nearly linearly with the distance from the center plane out to the top and bottom, but the accelerations are twice as large along the center axis as they are out at the rim of the disk. If we then add a guard ring and guard caps, the vertical component of the self-gravity accelerations become smaller, more linear, and more uniform. The guard caps used are large ones, 25 cm thick on the top and bottom of the disk. Instead of also using a large guard ring, however, we carefully pick a guard ring that is 10 cm thick, but only 4.5 cm wide. As we can see in the middle curves of Fig. 9, this leaves a variation in amplitude between the center of the disk and the rim of the disk.

To cancel this vertical component of self-gravity, we place the two 100-kg gravity gradient generator masses 58.18 cm above and below the guarded sample disk. The generator masses stay fixed relative to the inertially stabilized sample disk (while the six compensator masses rotate about the disk and its masses). Because of our choice for the

guard ring width, the acceleration fields of the self-gravity and the generator masses match so well that the resultant residual vertical acceleration field is found to be less than 1.3 picogravities. This is a factor of 2000 times smaller than the 3-nano-gravity self-field of the disk alone.

We must now cancel the horizontal components of the self-gravity. As we see in Fig. 10, because of the large guard caps used, the inward horizontal accelerations have increased in magnitude to  $-5.5$  nanogravities. In addition, the gravity gradient generator masses add their own inward horizontal accelerations of about  $-1$  nanogravity. Although both the self-gravity field and the generator field vary over the sample volume by about 40 picogravities, their variations are nearly equal and opposite in sign. Thus, when the two acceleration fields are combined, the combined field is almost perfectly linear with distance from the central axis. We can now compensate this field by rotating the sample with a period of about 9705.5 sec (2.7 h). As we see in the expanded scale in Fig. 10, the outward centrifugal acceleration cancels the inward gravitational acceleration to better than 0.8 picogravities, or a factor of nearly 4000 improvement over the original self-gravity field.

Thus, by going to geostationary orbit, canceling the residual background gravity gradients with a

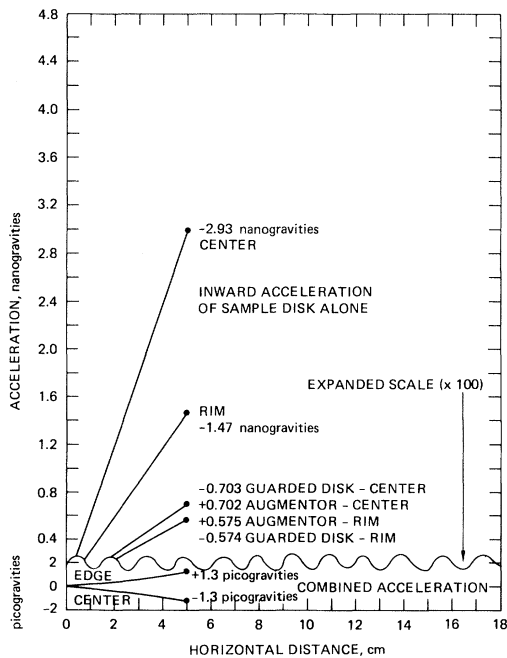


FIG. 9. Vertical accelerations in sample disk at geostationary orbit altitude.

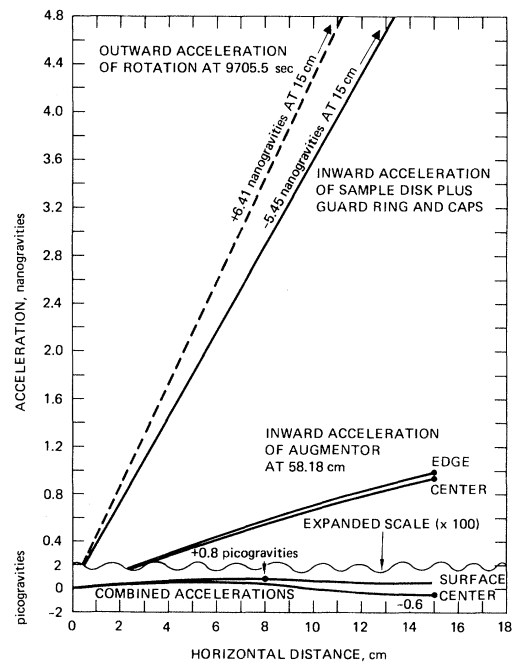


FIG. 10. Horizontal accelerations in sample disk at geostationary orbit altitude.

ring of six masses, and adjusting the field inside the sample volume with guard rings and guard caps, we can then use a two-mass gravity gradient generator and rotation to cancel the remaining gravity in a significant sample volume by factors of over 1000 to picogravity levels and below.

### XI. FLATTENING SPACETIME

From the point of view of general relativity, there is no such thing as a gravity field. The gravity potential and its derivatives, the gravity attractive force and the gravity gradient tides, are just

manifestations of the Riemann curvature of spacetime produced by nearby masses.<sup>7</sup> Since by the use of our gravity-compensation techniques we have found methods to reduce the gravity-induced accelerations over large regions, then the lack of residual accelerations implies that we have “flattened” that region of spacetime, despite the attempts of the mass of the Earth and the mass of the experiment itself to curve that spacetime.

One would think that there would be a good scientific use for a chunk of flat space the size of a hatbox, but except for the gravitation clock experiment, I have not thought of one (yet).

---

<sup>1</sup>R. E. Olsen and J. Mockovciak, Jr., *J. Spacecr. Rockets* 18, 141 (1981). [Olsen and Mockovciak wish to take this opportunity to make a minor correction in their paper. On p. 141, the last sentence of the next to last paragraph should read: “The maximum total acceleration per meter is  $2(\omega^2/9.8)$ .”]

<sup>2</sup>Staff of the John Hopkins APL Space Department and Staff of the Stanford Guidance and Control Laboratory, *J. Spacecr. Rockets* 11, 637 (1974.) (This paper also mentions the use of a single mass to compensate for residual gravity accelerations due to the spacecraft mass.)

<sup>3</sup>R. L. Forward, *Analog Science Fiction/Science Fact*, 100, No. 4, 67 (1980).

<sup>4</sup>R. L. Forward, *Dragon’s Egg* (Ballantine, New York, 1980), pp. 338–343 (hardcover), pp. 302–306 (paperback).

<sup>5</sup>R. L. Forward, AAS Reprint 71–364, Proceedings of the AAS/AIAA Astrodynamics Specialists Conference, Ft. Lauderdale, Florida, 1971 (unpublished).

<sup>6</sup>W. D. MacMillan, *The Theory of the Potential* (Dover, New York, 1958), problem 4, p. 22.

<sup>7</sup>C. W. Misner, K. S. Thorne, and J. A. Wheeler, *Gravitation* (Freeman, San Francisco, 1973), Chap. 16.